• Clinical Research •

Alterations of interhemispheric functional connectivity in patients with hypertensive retinopathy using voxel-mirrored homotopic connectivity: a resting state fMRI study

Xue-Lin Wang[1], Yu Chen[2], Jin-Yu Hu[3], Hong Wei[3], Qian Ling[3], Liang-Qi He[3], Cheng Chen[3], Yi-Xin Wang[4], Yan-Mei Zeng[3], Xiao-Yu Wang[3], Qian-Min Ge[3], Xu Chen[5], Yi Shao[3,6]

[1]Department of Ophthalmology, the First Affiliated Hospital of Jiangxi Medical College, Shangrao Center Hospital, Eye Hospital of Shangrao City, Shangrao 334000, Jiangxi Province, China
[2]Department of Traditional Chinese Medicine, the Second Affiliated Hospital of Liaoning University of Traditional Chinese Medicine, Shenyang 110000, Liaoning Province, China
[3]Department of Ophthalmology, the First Affiliated Hospital of Nanchang University, Nanchang 330006, Jiangxi Province, China
[4]School of Optometry and Vision Science, Cardiff University, Cardiff, CF24 4HQ, Wales, UK
[5]Ophthalmology Centre of Maastricht University, Maastricht 6200MS, Limburg Provincie, the Netherlands
[6]Department of Ophthalmology, Shanghai General Hospital, Shanghai Jiao Tong University School of Medicine, National Clinical Research Center for Eye Diseases, Shanghai 200080, China
Co-first authors: Xue-Lin Wang and Yu Chen
Correspondence to: Yi Shao. Shanghai General Hospital, Shanghai Jiao Tong University School of Medicine, National Clinical Research Center for Eye Diseases, Shanghai 200080, China. freebee99@163.com; Yi-Xin Wang. School of Optometry and Vision Science, Cardiff University, Cardiff, CF24 4HQ, Wales, UK. 731579475@qq.com
Received: 2023-11-25 Accepted: 2024-11-30

Abstract

● **AIM:** To analyze whether alterations of voxel mirror homology connectivity (VMHC) values, as determined by resting-state functional magnetic resonance imaging (rs-fMRI), occur in cerebral regions of patients with hypertensive retinopathy (HR) and to determine the relationship between VMHC values and clinical characteristics in patients with HR.

● **METHODS:** Twenty-one patients with HR and 21 age-matched healthy controls (HCs) were assessed by rs-fMRI scanning. The functional connectivity between the hemispheres of the cerebrum was assessed by measuring VMHC, with the ability of VMHC to distinguish between the HR and HC groups assessed using receiver operating characteristic (ROC) curve analysis. Differences in the demographic and clinical characteristics of the HR and HC groups were analyzed by independent sample *t*-tests. The relationship between average VMHC in several brain areas of HR patients and clinical features was determined using Pearson correlation analysis.

● **RESULTS:** Mean VMHC values of the bilateral cuneus gyrus (BA19), bilateral middle orbitofrontal gyrus (BA47), bilateral middle temporal gyrus (BA39) and bilateral superior medial frontal gyrus (BA9) were lower in the HR than in the HC group.

● **CONCLUSION:** VMHC values can predict the development of early HR, prevent the transformation of hypertensive microangiopathy, and provide useful information explaining the changes in neural mechanism associated with HR.

● **KEYWORDS:** hypertensive retinopathy; voxel-mirrored homotopic connectivity; neuroimaging; functional MRI; resting state

DOI:10.18240/ijo.2025.02.14

Citation: Wang XL, Chen Y, Hu JY, Wei H, Ling Q, He LQ, Chen C, Wang YX, Zeng YM, Wang XY, Ge QM, Chen X, Shao Y. Alterations of interhemispheric functional connectivity in patients with hypertensive retinopathy using voxel-mirrored homotopic connectivity: a resting state fMRI study. *Int J Ophthalmol* 2025;18(2):297-307

INTRODUCTION

Hypertension, defined as a persistent increase in systemic arterial blood pressure, is a common clinical syndrome that can lead to changes in the heart, brain, kidney and blood vessels, as well as being associated with the progression of

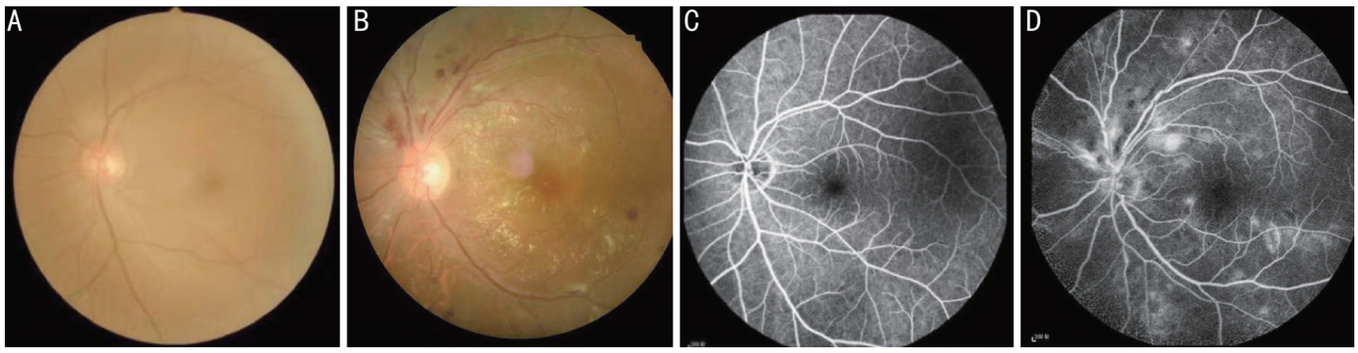

Figure 1 Typical examples of fundus camera and fluorescence fundus angiography in healthy people and patients with HR A, C: The left retinal fundus photos and corresponding fluorescence fundus angiography of healthy people; B, D: The left retinal fundus photos and fluorescence fundus angiography of patients with HR. Retinal arteriosclerosis, stenosis, wall light reflection enhancement, silver filiform, artery and vein cross compression phenomenon, the distal vein and capillary dilatation, retinal edema, bleeding and exudation. HR: Hypertensive retinopathy.

potentially blinding vascular disease of the eye. Increases in blood pressure induce a series of pathophysiological changes in the retina, leading to clinical symptoms called hypertensive retinopathy (HR)[1]. Early-stage HR is characterized by arteriosclerosis of the central retinal artery on fundus examination. Weakened elasticity of the arteriolar wall, increased fragility, and subsequent expansion, rupture, and hemorrhage are common after hyaline degeneration of the small arteries. Visible blood vessels may become convoluted, with enhanced reflection and an indentation at the artery-vein intersection. Severe HR can result in optic disc edema, retinal hemorrhage, and vision loss[2-3] (Figure 1).

Depending on age, the degree of elevated blood pressure, and the course of the disease, over 70% of patients with primary hypertension will develop HR of varying degrees[4]. About 6% to 15% of nondiabetic adults aged >40y show signs of HR, with HR being strongly associated with primary hypertension[5]. Moreover, HR and systemic hypertension are predictive of stroke, congestive heart failure and cardiovascular death independent of traditional risk factors. Similarly, hypertension can cause various retinal vascular and nonvascular ocular diseases, including retinal vein and arterial occlusion, ischemic optic neuropathy, glaucoma, and age-related macular degeneration[6].

Morphologically and physiologically, the large blood vessels and microvascular vessels that supply blood to the retina are similar to vessels that supply blood to the brain[7]. The retinal and cerebral vascular networks have similar vascular regulation processes, suggesting that changes in the retinal vasculature may reflect changes in cerebral blood vessels. Thus, patients with HR experience similar changes in the brain microvascular. Changes in the retinal arterial blood flow were found to be associated with cerebral arterial blood flow in spontaneously hypertensive rats, suggesting that changes in retinal arterial blood flow may predict cerebral arterial blood flow in hypertensive patients[8]. Patients with moderate HR, as indicated by cotton wool spots, retinal hemorrhages, and microaneurysms, were found to be at a 2- to 4-fold higher risk of stroke than patients without HR, after adjustment for age, gender, blood pressure, race, diabetes, and other risk factors for stroke. Signs of HR were also found to correlate with cognitive decline[9], white matter lesions on brain magnetic resonance imaging (MRI), lacunar infarction[10], brain atrophy[11], and stroke[12]. These findings indicate that, in addition to being an eye disease, HR is associated with the brain microcirculation, brain microvascular lesions, and changes in brain activity.

Functional magnetic resonance imaging fMRI is a blood oxygenation level dependent (BOLD)[13] functional brain imaging technique that can reveal brain activity and has been used to study HR and other diseases. Resting-state functional MRI (rs-fMRI), first described in 1995[14], has been used to evaluate human brain sensation, cognition, emotion, and disease mechanisms. Because rs-fMRI, which combines anatomical and functional imaging and does not induce radiation damage[13], has unique tracking and localization capabilities, this technique is frequently used to investigate the intrinsic neural activity of the brain at rest. The rs-fMRI method can detect changes in various brain regions and quantify these changes using various algorithms, enabling analysis of the potential impact of disease states on the brain and further investigation of the neuropathological mechanisms associated with these diseases. Current rs-fMRI analytical techniques are complex and diverse, involving a variety of methods for analyzing data. Several methods can be used to assess neural network functional connectivity (FC) and information flow in various regions of the brain, including seed-based FC, independent component analysis (ICA), and graph theory.

Visual experience is closely related to inter-hemispheric synchrony[15]. Visual perception may even be normal in

individuals with abnormalities in visual cortical anatomy. Voxel mirror homology connectivity (VMHC) is an analytical technique that can quantify interhemispheric FC between the time sequence of a given voxel in one hemisphere and its mirror correspondence in the other hemisphere[16]. VMHC has been widely used to study the relationship between eye diseases and abnormal brain activity, including in patients with post-herpetic neuralgia[17], unilateral retinal detachment[18], acute eye pain[19], diabetic nephropathy with retinopathy[20], corneal ulcer[21], and unilateral acute open eye injury[22]. However, it is unclear whether interhemispheric FC is abnormal in patients with HR. The present study hypothesized that the average VMHC value could be a useful clinicobiological marker for HR. Therefore, this study used the VMHC method to assess whether interhemispheric FC is altered in subjects with HR.

PARTICIPANTS AND METHODS

Ethical Approval The Medical Ethics Committee of the First Affiliated Hospital of Nanchang University approved this research, and we followed the relevant provisions of the declaration of Helsinki; at the same time, the enrolled patients who participated in the study were informed of the study purpose, procedures, and signed informed consent.

Participants From August 2020 to October 2022, we randomly selected 21 HR patients (11 males and 10 females) from the Department of Ophthalmology of the First Affiliated Hospital of Nanchang University. The following are the diagnostic criteria for HR: 1) Fundus examination based on systematic diagnosis of stage 2 or above hypertension (systolic blood pressure ≥140 mm Hg or diastolic blood pressure ≥90 mm Hg); 2) a record of microaneurysm, retinal hemorrhage, cotton thread spot, exudate, arteriovenous chiasm, arteriole stenosis, and papilledema to classify retinopathy. According to Keith-Wagener, retinopathy was graded as follows[3]: Grade I, mild retinal arterial stenosis or sclerosis; Grade II, moderate arterial stenosis with arteriovenous crossing; Grade III, arterial stenosis and large arteriovenous crossing changes with hemorrhage, Exudate and cotton spots; Grade IV, severe grade III with papilledema. Subject exclusion criteria were as follows: 1) history of eye surgery, diabetes, and/or neurological disease; 2) inability to perform MRI scans for subjective and objective reasons; 3) alcohol intake >30 g/day; 4) old or multiple cerebral infarctions in the MRI scan. We also recruited 21 healthy volunteers (11 males and 10 females) from different communities in Nanchang City, Jiangxi Province, China as a healthy control (HC) group, who were similar with the HR group in demographic information such as gender, age, and education level. Here is a list of criteria that all HCs met: 1) no ophthalmic or neurological disease; 2) normal brain parenchyma on head MRI scan; 3) no contraindications to MRI.

Magnetic Resonance Imaging Data Acquisition A Trio 3-Tesla MRI scanner (Siemens AG) was used for the MRI scans. All participants were examined by MRI on a 3.0T system which had eight-channel head coil (Siemens, Munich, Germany).

Under three-dimensional gradient recall sequence , high-resolution T1-weighted whole-brian scans were performed with the parameters: echo time=2.26ms, repetition time=1900ms, gap=0.5 mm, thickness=1.0 mm, acquisition matrix (AM) =256×256, flip angle (FA) =9°, field of view =250×250 mm). The functional data were collected using a 3D spoiled gradient-recalled echo sequence with the following parameters: echo time =30ms, repetition time =2000ms, gap =1.2 mm, thickess =4.0 mm, AM=64×64, FA=90°, 29 axial, field of view =220×220 mm), covered whole brain were corrected. They recline on the examination table, remain alert, close their eyes, unwind, breathe normally, attempt to avoid movement, and immobilise the subject's head with a spongy foam pad while inserting cotton balls into the subject's ears to reduce noise disruption and all scans were carried out by the same imaging doctor, who restrained head movement and watched the patients until the operation was fully achieved.

Data Processing The MRIcro programme on the Web (www.MRICRO.com) pre-filters the functional imaging data before acquisition. This is done using a technique called statistical parameter mapping (SPM12), which utilizes MATLAB code. 1) Signal balance and scan noise were taken into account during data gathering by removing the first 10 volumes of each participant. 2) All other images should be corrected for their little motions and time differences, and the signals captured at different times should be synchronized to the same time. 3) Improve the spatial accuracy of the normalised fMRI data by converting a single T1-weighted rapid gradient-echo structural picture that has undergone magnetization processing to average fMRI data, and then segmenting the resultant T1-weighted image using Dartel tools. 4) Exclude the head in x, subjects with >1.5 mm movement in y or z direction or >1.5° angular rotation (such as breathing and heartbeat). 6) Using a common echo-planar imaging template, we normalised the functional pictures to the Montreal Neurological Institute (MNI) spatial standard and smoothed them with a 4 mm×4 mm×4 mm full width at half maximum (FWHM) to comply with their space standards. 7) To lessen the impact of head motion and other signals, white matter and cerebrospinal fluid signals were regressed. 8) De-Line Drift: Removes the effects of higher machine temperatures or subject fatigue brought on by prolonged scanning.

Statistical Analysis in Voxel-mirrored Homotopic Connectivity The VMHC maps of the patients were

Table 1 Conditions of participants included in the study mean±SD

Condition	HR	HCs	*t*	*P*[a]
Male/female (M/F)	11/10	11/10	N/A	>0.99
Family history of hypertension (M/F)	6/5	N/A	N/A	N/A
Smoking status (M/F)	6/5	6/5	N/A	N/A
Age (y)	54.35±6.87	51.36±6.86	0.178	0.756
Weight (kg)	69.64±4.42	65.57±5.75	0.202	0.804
Handedness	21R	21R	N/A	>0.99
Duration of HR (y)	31.66±12.65	N/A	N/A	N/A
Best-corrected VA-left eye	0.66±0. 17	1.05±0.25	-3.764	0.007
Best-corrected VA-right eye	0.57±0.21	1. 10±0.20	-3.835	0.003
Confrontation VF	Full	Full	N/A	N/A
SBP (mm Hg)	166±25	116±18	9.037	<0.001
DBP (mm Hg)	101±15	76±11	2.142	0.016
CR (beats per minute)	69±12	62±14	0.825	0.067

[a]*P*<0.05. Independent *t*-tests comparing two groups. DBP: Diastolic blood pressure; HR: Hypertensive retinopathy; CR: Cardiac rate; HCs: Normal controls; VA: Visual acuity; N/A: Not applicable; SBP: Systolic blood pressure; VF: Visual field.

Table 2 Brain areas demonstrated significantly different VMHC values between HR and HC group

Brain areas	MNI coordinates						ROI
	X	Y	Z	BA	Peak voxels	T	
HC>PAT							
Cuneus_R	6	-90	24	19	524	-3.88	Cluster 1
Cuneus_L	-6	-90	24	19	524	-3.88	Cluster 2
Temporal_Mid_R	45	-69	51	39	92	-3.66	Cluster 3
Temporal_Mid_L	-45	-69	51	39	92	-3.66	Cluster 4
Frontal_Sup_Medial_R	15	57	12	9	81	-3.45	Cluster 5
Frontal_Sup_Medial_L	-15	57	12	9	81	-3.45	Cluster 6
Frontal_Med_Orb_R	9	30	-12	47	108	-3.28	Cluster 7
Frontal_Med_Orb_L	-9	30	-12	47	108	-3.28	Cluster 8

VMHC: Voxel-mirrored homotopic connectivity; HR: Hypertensive retinopathy; HC: Healthy control; BA: Brodmann area; MNI: Montreal Neurological Institute; PAT: Patient; ROI: Region of Interest; L: Left; R: Right; Cuneus_R: Right Cuneus; Cuneus_L: Left Cuneus; Frontal_Med_Orb_R: Right medial orbitofrontal gyrus; Frontal_Med_Orb_L: Left medial orbitofrontal gyrus; Temporal_Mid_R: Right middle temporal gyrus; Temporal_Mid_L: Left middle temporal gyrus; Frontal_Sup_Medial_R: Right medial superior frontal gyrus; Frontal_Sup_Medial_L: Left medial superior frontal gyrus.

transformed to z-values using Fisher z-transformations in the REST programme (http://resting-fmri.sourceforge.net) to standardise the data. By utilizing global VMHC as a covariate for each voxel, two-sample *t*-tests were conducted to compare VMHC values between the two groups. Statistical comparisons were made at the voxel level ($P<0.05$), based on Gaussian random field theory (cluster >54 voxels, $P>0.01$, AlphaSim corrected). These voxels were chosen as the areas of interest where remarkable differences between the two groupings could be found.

Statistical Analysis Statistical analysis of significant data was performed using SPSS Version 25.0 (SPSS Inc., Chicago, IL, USA). The SPM12 toolset was used to run two-sample *t*-tests to determine if the HR and HC groups' VMHC z-plots differed from one another. The average VMHC in each group's respective brain areas was calculated using the receiver operating characteristic (ROC) curve approach.

Brain-Behavior Correlation Analysis Using REST software, several areas of interest in the HR group's brain were identified based on their differing VMHC levels. GraphPad Prism7 (GraphPad Software Inc., San Diego, CA, USA) was used to conduct a Pearson correlation analysis to clarify the connection between mean VMHC values in various brain areas and behavioural performance. Statistics were judged significant at $P<0.05$.

RESULTS

Demographic and visual characteristics of the study population were shown in Table 1.

Voxel-Mirrored Homotopic Connectivity Differences VMHC values in the bilateral cuneus (BA19), bilateral medial orbital frontal gyrus (BA47), bilateral middle temporal gyrus (BA39), and bilateral medial superior frontal gyrus (BA9) were lower in patients with HR than in HCs (Figure 2, Table 2). A histogram showed the between-group differences in mean

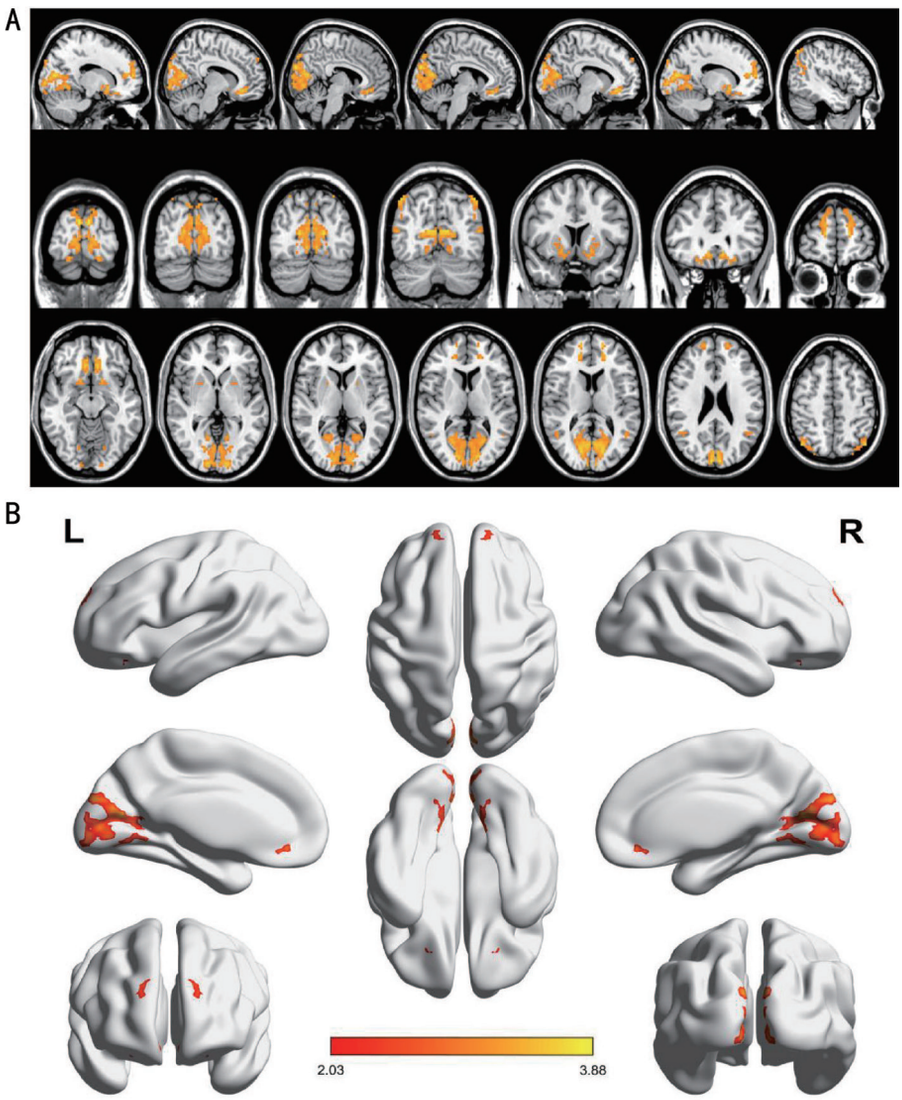

Figure 2 Significant differences in VMHC values between the HR and HC group Differences of the VMHC values were seen in the cuneus gyrus (R/L), medial orbital frontal gyrus (R/L), middle temporal gyrus (R/L) and medial superior frontal gyrus (R/L). Lower VMHC values were shown in blue or purple (P<0.01 for multiple comparisons using GRF theory). VMHC: Voxel-mirrored homotopic connectivity; HR: Hypertensive retinopathy; HC: Healthy control; BA: Brodmann's area; GRF: Gaussian random field.

VMHC values in several brain regions (Z>2.3, P<0.01, cluster 54 voxels with AlphaSim corrected; Figure 3).

Correlation Analysis Analysis of patients with HR showed that their clinical symptoms did not correlate significantly with VMHC values in various areas of the brain (P>0.05 each).

Receiver Operating Characteristic Curve Analysis This study had hypothesized that differences in VMHC values between the HR and HC groups may be a diagnostic indicator distinguishing between these two groups. Mean VMHC values in various parts of the brain of these two groups were therefore compared using receiver operating characteristic (ROC) curve analysis, with higher areas under the curve (AUC) indicating a greater difference between the two groups. The AUCs were 0.845 [P<0.0001; 95% confidence interval (CI) 0.701–0.990] for both the right and left sided cuneus gyrus (BA19), 0.812 (P<0.0001; 95%CI 0.674–0.951) for both the right and left sided medial orbitofrontal cortex (BA47), 0.836 (P<0.0001; 95%CI 0.684–0.989) for both the right and left sided middle temporal gyrus (BA39), and 0.827 (P<0.0001; 95%CI 0.692–0.963) for both the right and left sided superior medial frontal gyrus (BA9, Figure 4).

DISCUSSION

VMHC, a somewhat new measure that can reflect interhemispheric FC changes in the brain, has been used in the diagnosis of several ophthalmologic conditions (Table 3). To our knowledge, however, the present study is the first to use VMHC to assess cross-hemispheric FC in patients with HR. This study found that VMHC values in the bilateral medial superior frontal gyrus, bilateral medial orbitofrontal cortex, bilateral middle temporal gyrus, and bilateral cuneus were significantly lower in the HR than in the HC group (Figure 5).

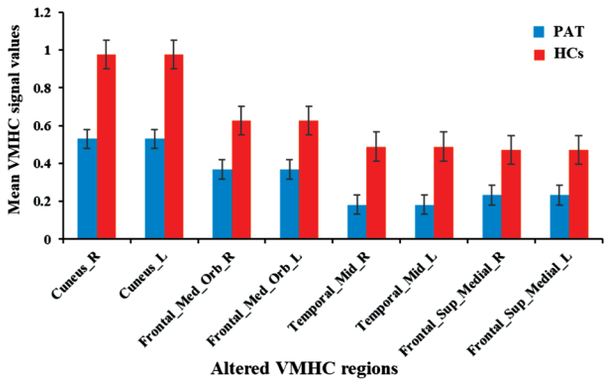

Figure 3 The mean VMHC values of significant brain regions between HR group and HC group VMHC: Voxel-mirrored homotopic connectivity; HR: Hypertensive retinopathy; PAT: Patient; HC: Healthy control; L: Left; R: Right; Cuneus_R: Right Cuneus; Cuneus_L: Left Cuneus; Frontal_Med_Orb_R: Right medial orbitofrontal gyrus; Frontal_Med_Orb_L: Left medial orbitofrontal gyrus; Temporal_Mid_R: Right middle temporal gyrus; Temporal_Mid_L: Left middle temporal gyrus; Frontal_Sup_Medial_R: Right medial superior frontal gyrus; Frontal_Sup_Medial_L: Left medial superior frontal gyrus.

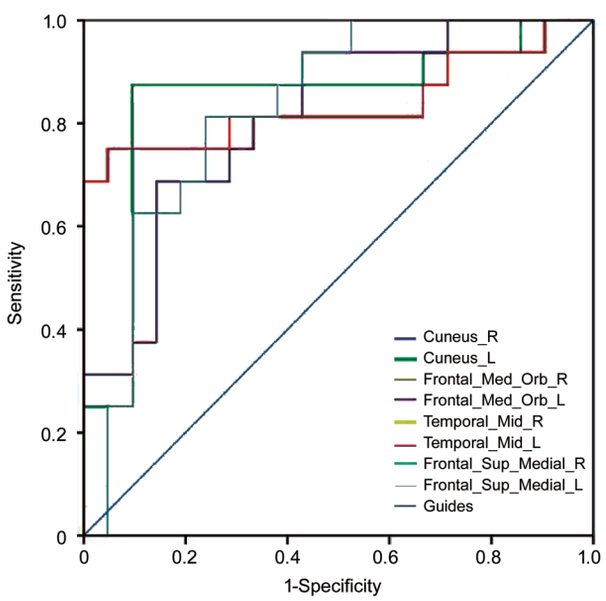

Figure 4 ROC curve analysis of the mean VHMC values for altered brain regions The area under the ROC curve were 0.845 (P<0.0001; 95%CI: 0.701–0.990) for Cuneus_R, Cuneus_L 0.845 (P<0.0001; 95%CI: 0.701–0.990), Frontal_Med_Orb_R 0.812 (P<0.0001; 95%CI: 0.674–0.951), Frontal_Med_Orb_L 0.812 (P<0.0001; 95%CI: 0.674–0.951), Temporal_Mid_R 0.836 (P<0.0001; 95%CI: 0.684–0.989), Temporal_Mid_L 0.836 (P<0.0001; 95%CI: 0.684–0.989), Frontal_Sup_Medial_R 0.827 (P<0.0001; 95%CI: 0.692–0.963), Frontal_Sup_Medial_L 0.827 (P<0.0001; 95%CI: 0.692–0.963). AUC: Area under the curve; ROC: Receiver operating characteristic; VMHC: Voxel-mirrored homotopic connectivity; CI: Confidence interval; HRP: Hypertensive retinopathy; HC: Healthy control. Cuneus_R: Right Cuneus; Cuneus_L: Left Cuneus; Frontal_Med_Orb_R: Right medial orbitofrontal gyrus; Frontal_Med_Orb_L: Left medial orbitofrontal gyrus; Temporal_Mid_R: Right middle temporal gyrus; Temporal_Mid_L: Left middle temporal gyrus; Frontal_Sup_Medial_R: Right medial superior frontal gyrus; Frontal_Sup_Medial_L: Left medial superior frontal gyrus.

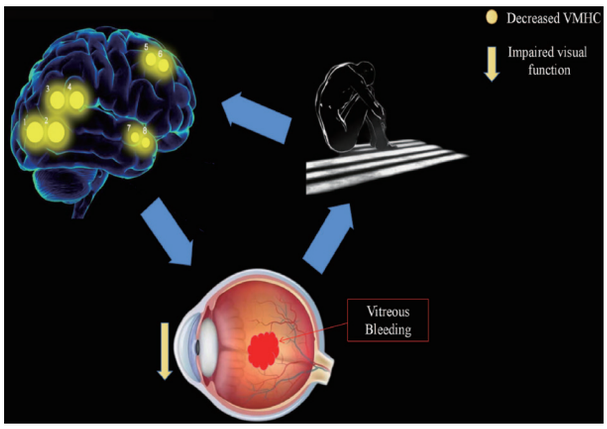

Figure 5 The mean VHMC values of altered brain regions in the hypertensive retinopathy group The VHMC values of the following regions were reduced to varying degrees when compared to the HCs: 1-Cuneus_R (BA 19, t=-3.88), 2-Cuneus_L (BA 19, t=-3.88), 3-Temporal_Mid_R (BA 39, t=-3.66), 4-Temporal_Mid_L (BA 39, t=-3.66), 5-Frontal_Sup_Medial_R (BA 39, t=-3.45), 6-rontal_Sup_Medial_L (BA 39, t=-3.45) , 7-Frontal_Med_Orb_R (BA 47, t=-3.28), 8-Frontal_Med_Orb_L (BA 47, t=-3.28). The sizes of the spots denote the degree of quantitative changes. VMHC: Voxel-mirrored homotopic connectivity; HC: Healthy control; L: Left: R: Right; BA: Brodmann's area. Cuneus_R: Right Cuneus; Cuneus_L: Left Cuneus; Frontal_Med_Orb_R: Right medial orbitofrontal gyrus; Frontal_Med_Orb_L: Left medial orbitofrontal gyrus; Temporal_Mid_R: Right middle temporal gyrus; Temporal_Mid_L: Left middle temporal gyrus; Frontal_Sup_Medial_R: Right medial superior frontal gyrus; Frontal_Sup_Medial_L: Left medial superior frontal gyrus.

Table 3 Voxel-mirrored homotopic connectivity method applied in ophthalmological diseases

Author (y)	Disease	References
Peng *et al* (2021)	Retinal detachment	18
Dong *et al* (2019)	Acute eye pain	19
Shi *et al* (2019)	Corneal ulcer	20
Wang *et al* (2020)	Diabetic nephropathy and retinopathy	21

The cuneus (BA19) is located on the medial side of the occipital lobe, between the parietooccipital sulcus and the posterior part of the calcarine sulcus. The lateral geniculate body of the thalamus transmits retinal information to the primary visual cortex (V1), also called the striate cortex, in the visual pathway. Interactions between the V1 and the anteromedial cuneus encode visual information for the extrastriate cortex (V2-V4). The cuneus is involved in spatial localization (stereoscopic vision)[23], as well as in object recognition[24]. The cuneus has many local connections[25], enabling coordinated basic visual processing, such as spatial frequency, orientation, motion, and velocity[26]. Simultaneously, because the cuneus is the hub of many long-distance connecting fibers, it has functions other than basic visual processing[27], such as multimodal semantic processing,

visual memory, emotional facial expression processing, and face recognition[28]. Increase gray matter volume in the cuneus was shown to correlate with a greater degree of creative thinking, indicating that the cuneus plays a role in visual imagination[29]. In individuals with impaired vision, the cuneus can promote cross-modal, non-visual functions, like verbal memory and language processing. A Meta-analysis of 166 children who became blind before age 6y revealed that the cuneus is activated during language processing tasks, such as Braille reading, sentence completion, and verbal memory[30]. HR was shown to correlate positively with AS in HR patients with elevated cuneus DC values (anxiety), suggesting that the cuneus lobe of HR patients undergoes compensatory visual processing after visual dysfunction[31]. These patients may later experience anxiety due to their difficulty recovering the vision expected.

The bilateral visual cortex of normal individuals has been shown to exhibit stable isochronous FC during resting states. In contrast, the present study found that VMHC values in the cuneus were lower in patients with HR than in HCs, indicating that the interhemispheric FC of the cuneus was affected in patients with HR. This change in FC may be due to a reduction of visual cortical stimulation after impairment of visual function in patients with HR. Furthermore, the impaired bilateral coordination of the cuneus in patients with HR may result in defects in visual pathways, leading to visual processing dysfunction. An abnormal interhemispheric FC value in HR patients may be a useful clinical indicator for assessing visual information processing.

The orbitofrontal cortex[32], which is located the anterior cranial fossa above the orbit, consists of a large cortex on the ventral side of the frontal lobe. The sulcus, medial orbitofrontal sulcus, lateral orbitofrontal sulcus, and transverse orbital sulcus are divided into the gyrus rectus, medial orbitofrontal cortex (mOFC), anterior orbitofrontal gyrus cortex (aOFC), lateral orbitofrontal cortex (lOFC) and posterior orbitofrontal cortex (pOFC), roughly corresponding to BA 10,11, 12, 13, 14, and 47, respectively. The fiber connections of the OFC are extremely complicated, with functional differences between the medial and lateral regions, as well as between the anterior and posterior regions, of the OFC. The lOFC primarily receives sensory cortex input, including somatosensory, visual and gustatory information. The mOFC is closely related to the ventromedial prefrontal lobe, as well as the hypothalamus, periaqueduct gray matter, and amygdala, and is associated with information processing of, for example, visceral sensations, emotions, and rewards[33]. The mOFC also plays an important role in regulating effort-related motivational functions, with damage to the mOFC leading to decreased motivation, which further affects learning and memory[34].

The OFC has been linked to the regulation of autonomic nervous responses, self-monitoring, reward mechanisms[35], decision-making[36], learning, memory, emotion[37], and motivation[34], as well as the regulation of social behavior and mental state. Impairment of the OFC causes significant emotional changes and plays an important role in regulating human emotions. Increased activity of the medial orbitofrontal cerebral zone has been associated with the presentation of positive affect, whereas decreased activity of the medial orbitofrontal cerebral zone has been found to correlate with tempering of favorable affect[38]. Moreover, impairment of the OFC was found to impair emotion-related learning, affective behavior, and subjective affective states[37], as well as leading to exaggerated emotional experiences and neuropsychiatric disorders[39]. FC in the IOFC was found to be increased, whereas FC in the mOFC was decreased, in patients with depression. In addition, voxel-based morphometry of gray matter volume in children showed that OFC morphology plays an important role in depression processes, indicating early symptoms of depression before the development of clinically significant depression[40]. Lesions in the orbitofrontal cortex are frequently linked to behavioral syndromes characterized by episodic symptoms (*e.g.*, insensitivity and decreased interest and motivation), exploitative and imitative behaviors, personality changes (*e.g.*, disinhibition and emotional instability), and reversal of impaired learning and anticipatory memory.

Assessment of the associations between local brain activity features and clinical traits showed that the amplitude of low-frequency fluctuation (ALFF) of the OFC was lower in patients with dry eye (DE) than in controls. These findings suggested that the decreased local activity of the OFC in patients with DE could lead to depression. The present study showed that VMHC values in the bilateral OFC were lower in HR patients than in HCs, suggesting that impaired OFC could lead to poorer mental and emotional states, decreased inhibitory control, and affective passivation. The relationship between lower VMHC values and depression mechanisms in HR patients should also be considered, as HR may cause depressive symptoms by damaging the OFC, which, in turn, could cause VMHC changes.

The middle temporal gyrus (MTG, BA39) is a brain gyrus between the superior temporal sulcus and the inferior temporal sulcus. The MTG can be divided into four regions based on differences in anatomical connection characteristics[41]: the anterior middle temporal gyrus (AMTG), the middle porch temporal gyrus (MMTG), the posterior middle temporal gyrus (PMTG), and the sulcus middle temporal gyrus (SMTG). Anatomically and functionally, these four MTG subregions exhibit different patterns of connectivity.

The primary functions of the AMTG include default mode networks, voice recognition, semantic extraction, and language understanding[42]. The main functions of the MMTG include semantic memory and semantic control networks. The PMTG is strongly connected to language-related regions, suggesting that the PMTG could be a semantic hub[43]. Finally the SMTG is linked to gaze direction decoding as well as understanding spoken language[41].

By utilizing contextual knowledge content to extract semantic information related to visual and auditory information, the MTG is believed to be involved in cognitive processes related to language, such as lexical comprehension[44] and semantic cognition[45]. The PMTG plays an important role in semantic cognition[46], with the MTG being activated during the performance of language-related functions[47]. The MTG was found to be involved in two distinct coherent resting-state networks, the default mode (DMN) and semantic memory (SM) networks[48]. The gray matter volume in the left MTG was found to be lower in patients with proliferative diabetic retinopathy (PDR) than in controls, with this decrease in gray matter volume suggesting neuronal loss and atrophy in patients with DR[49].

The present study also found that VMHC values were lower in the contralateral middle temporal gyrus of patients with HR than in HCs, suggesting that semantic cognitive function is lower in patients with HR. These lower VMHC values may be an imaging marker for the diagnosis of HR, suggesting that rs-fMRI may provide a new diagnostic technique for clinical screening of HR.

The medial superior frontal gyrus (mSFG; BA9) is positioned anterior to the paracentral lobule and passes forward through the cingulate gyrus, encompassing the medial BA8 and BA9 areas[50]. The medial frontal cortex (MFC) was shown to be an essential component of interactive social behavior[51], called the "social brain", as it is a node in a brain network that monitors social behavior[52]. The MFC also serves as a cortical node for the wider limbic system. In addition to being involved in the control of intricate social behaviors, the MFC is also involved in several types of non-social behaviors, including rewards, emotions, higher executive function, and decision processing, suggesting that the MFC performs several fundamental functions in internally directing cognition[53]. The MFC participates in the executive control network, as well as being involved in cognitive control, working memory, goal-directed activities, and intellectual activity control MFC[13]. The BA8 area of the medial frontal gyrus includes the frontal visual field (FEF), which is involved in spatial sustained attention[54] and eye movement[55], and plays a critical role in saccade. Damage to this region can lead to eye movement abnormalities. Indeed, diffusion tensor imaging showed that fractional anisotropy (FA) of the medial frontal gyrus was lower in patients with strabismus than in normal controls, indicating that the MFC was associated with strabismus[56].

The prefrontal cortex is split into four regions: the medial, dorsolateral, ventrolateral, and polar regions[57]. The medial prefrontal cortex includes the mSFG. The DMN was found to include the posterior cingulate cortex, middle prefrontal cortex, and bilateral temporopariietal junction (TPJ), indicating that the mSFG is part of the DMN[58]. The DMN was found to consist of numerous parallel interleaved networks with specialization in juxtaposed places, rather than being a single network, as previously thought[59]. In addition to being task-negative, the DMN is active only when an individual is resting, becoming inactive when the individual performs an external task. Due to its involvement in social cognition, such as engaging in introspection, mind wandering, emotional processing, or imagining another individual's mental state, this network has been referred to as a mind network[13]. The DMN should not be regarded as an internal network that is exclusively active in response to inputs that are either internally directed or independent. Rather, the DMN should be regarded as a dynamic, active "sense-making" network that connects the external world with the inner world. This network may integrate external and internal information, allowing social cognition, self-awareness, and better adaptation to various environmental changes. The DMN may also play a role in cognitive skills, including anticipatory and situated memory, decision making, social reasoning, and self-produced thinking[60]. The DMN may also be associated with depression[61], mild cognition[62], and other disorders.

Brain areas affected by HR have been assessed using ALFF, as have the links between ALFF values and underlying emotional and psychological changes[63]. Compared with HCs, patients with HR patients had much lower left SFG ALFF values, suggesting that HR may lead to damage to the DMN, with this damage possibly leading to depressive symptoms. The present study found that VMHC values were significantly lower in the bilateral mSFG of patients with HR, suggesting that HR may cause cognitive dysfunction, with the accompanying disruption of the DMN resulting in depressive symptoms. These findings indicate the need for increased psychological therapy and nursing care in patients with HR. The lower VMHC values at the mSFG in patients with HR suggest that HR may limit voluntary eye movement. Thus, these lower VMHC values of the mSFG may reflect eye movement dysfunction in patients with HR.

Based on our findings above, we constructed a table of the functions corresponding with various brain region, and the effects of alterations associated with HR on functional activities (Table 4).

Table 4 Changes in specific brain regions and their potential functional effects

Brain regions	Experimental result	Brain function	Anticipated results
Cuneus_R	HRs<HCs	Spatial localization, object recognition and visual processing	Impaired bilateral coordination, visual processing dysfunction.
Cuneus_L	HRs<HCs	Spatial localization, object recognition and visual processing	Impaired bilateral coordination, visual processing dysfunction.
Temporal_Mid_R	HRs<HCs	Lexical comprehension, semantic cognition	Disorder of the semantic cognitive function
Temporal_Mid_L	HRs<HCs	Lexical comprehension, semantic cognition	Disorder of the semantic cognitive function
Frontal_Sup_Medial_R	HRs<HCs	Controls spontaneous eye movements, part of the default model network	Mental disorders, including depression and anxiety
Frontal_Sup_Medial_L	HRs<HCs	Controls spontaneous eye movements, part of the default model network	Mental disorders, including depression and anxiety
Frontal_Med_Orb_R	HRs<HCs	Rewards and decision-making human executive functions	Blunted positive affection, depression
Frontal_Med_Orb_L	HRs<HCs	Rewards and decision-making human executive functions	Blunted positive affection, depression

HR: Hypertensive retinopathy; HC: Healthy control; Cuneus_R: Right Cuneus; Cuneus_L: Left Cuneus; Frontal_Med_Orb_R: Right medial orbitofrontal gyrus; Frontal_Med_Orb_L: Left medial orbitofrontal gyrus; Temporal_Mid_R: Right middle temporal gyrus; Temporal_Mid_L: Left middle temporal gyrus; Frontal_Sup_Medial_R: Right medial superior frontal gyrus; Frontal_Sup_Medial_L: Left medial superior frontal gyrus.

In conclusion, the present study found that VMHC values in different areas of the cerebral hemisphere were significantly lower in patients with HR than in HCs, suggesting that VHMC may be useful for investigating the link between HR and interhemispheric connections. Aberrant VMHC levels in these brain regions may be biomarkers of impaired interhemispheric connectivity during early HR. Thus, rs-fMRI in patients can predict the development of HR, allowing the introduction of measures to prevent the transformation of hypertensive microangiopathy. Investigations of the etiology and pathology of HR have improved the ability to diagnose and treat this disease, Additional studies, however, are requires to confirm these results.

ACKNOWLEDGEMENTS

Foundations: Supported by National Natural Science Foundation of China (No.82160195; No.82460203).

Conflicts of Interest: Wang XL, None; **Chen Y,** None; **Hu JY,** None; **Wei H,** None; **Ling Q,** None; **He LQ,** None; **Chen C,** None; **Wang YX,** None; **Zeng YM,** None; **Wang XY,** None; **Ge QM,** None; **Chen X,** None; **Shao Y,** None.

REFERENCES

1 di Marco E, Aiello F, Lombardo M, *et al*. A literature review of hypertensive retinopathy: systemic correlations and new technologies. *Eur Rev Med Pharmacol Sci* 2022;26(18):6424-6443.

2 Modi P, Arsiwalla T. Cranial Nerve III Palsy. *StatPearls*. StatPearls Publishing Copyright© 2024, StatPearls Publishing LLC.; 2024.

3 Singh RB, Saini C, Shergill S, *et al*. Window to the circulatory system: ocular manifestations of cardiovascular diseases. *Eur J Ophthalmol* 2020;30(6):1207-1219.

4 Liu L, Quang ND, Banu R, *et al*. Hypertension, blood pressure control and diabetic retinopathy in a large population-based study. *PLoS One* 2020;15(3):e0229665.

5 Cheung CY, Biousse V, Keane PA, *et al*. Hypertensive eye disease. *Nat Rev Dis Primers* 2022;8(1):14.

6 Tsokolas G, Tsaousis KT, Diakonis VF, *et al*. Optical coherence tomography angiography in neurodegenerative diseases: a review. *Eye Brain* 2020;12:73-87.

7 Wiseman SJ, Zhang JF, Gray C, *et al*. Retinal capillary microvessel morphology changes are associated with vascular damage and dysfunction in cerebral small vessel disease. *J Cereb Blood Flow Metab* 2023;43(2):231-240.

8 Dziedziak J, Zaleska-Żmijewska A, Szaflik JP, *et al*. Impact of arterial hypertension on the eye: a review of the pathogenesis, diagnostic methods, and treatment of hypertensive retinopathy. *Med Sci Monit* 2022;28:e935135.

9 Tsukikawa M, Stacey AW. A review of hypertensive retinopathy and chorioretinopathy. *Clin Optom* 2020;12:67-73.

10 Rim TH, Teo AWJ, Yang HHS, *et al*. Retinal vascular signs and cerebrovascular diseases. *J Neuroophthalmol* 2020;40(1):44-59.

11 Chen MJ, Wu SN, Shu HY, *et al*. Spontaneous functional changes in specific cerebral regions in patients with hypertensive retinopathy: a resting-state functional magnetic resonance imaging study. *Aging* 2021;13(9):13166-13178.

12 Zhuo YY, Gao WH, Wu ZL, *et al*. Evaluating retinal blood vessels for predicting white matter hyperintensities in ischemic stroke: a deep learning approach. *J Stroke Cerebrovasc Dis* 2024;33(12):108070.

13 Smitha KA, Akhil Raja K, Arun KM, *et al*. Resting state fMRI: a review on methods in resting state connectivity analysis and resting state networks. *Neuroradiol J* 2017;30(4):305-317.

14 Canario E, Chen D, Biswal B. A review of resting-state fMRI and its use to examine psychiatric disorders. *Psychoradiology* 2021;1(1):42-53.

15 Huang X, Zhou FQ, Dan HD, *et al*. Impaired interhemispheric synchrony in late blindness. *Acta Radiol* 2020;61(3):414-423.

16 Cheng Y, Chen XL, Shi L, *et al*. Abnormal functional connectivity between cerebral hemispheres in patients with high myopia: a resting FMRI study based on voxel-mirrored homotopic connectivity. *Front Hum Neurosci* 2022;16:910846.

17 Zhang S, Gao GP, Shi WQ, *et al*. Abnormal interhemispheric functional connectivity in patients with strabismic amblyopia: a resting-state fMRI study using voxel-mirrored homotopic connectivity. *BMC Ophthalmol* 2021;21(1):255.

18 Peng JX, Yao F, Li QY, *et al*. Alternations of interhemispheric functional connectivity in children with strabismus and amblyopia: a resting-state fMRI study. *Sci Rep* 2021;11(1):15059.

19 Dong ZZ, Zhu FY, Shi WQ, *et al*. Abnormalities of interhemispheric functional connectivity in individuals with acute eye pain: a resting-state fMRI study. *Int J Ophthalmol* 2019;12(4):634-639.

20 Shi WQ, Liu JX, Yuan Q, *et al*. Alternations of interhemispheric functional connectivity in corneal ulcer patients using voxel-mirrored homotopic connectivity: a resting state fMRI study. *Acta Radiol* 2019;60(9):1159-1166.

21 Wang Y, Wang XY, Chen WZ, *et al*. Brain function alterations in patients with diabetic nephropathy complicated by retinopathy under resting state conditions assessed by voxel-mirrored homotopic connectivity. *Endocr Pract* 2020;26(3):291-298.

22 Ye L, Wei R, Huang X, *et al*. Reduction in interhemispheric functional connectivity in the dorsal visual pathway in unilateral acute open globe injury patients: a resting-state fMRI study. *Int J Ophthalmol* 2018;11(6):1056-1060.

23 Funayama M, Hojo T, Nakagawa Y, *et al*. Investigating the link between subjective depth perception deficits and objective stereoscopic vision deficits in individuals with acquired brain injury. *Cogn Behav Neurol* 2024;37(2):82-95.

24 Jiang YJ, Lai PH, Huang X. Interhemispheric functional in age-related macular degeneration patient: a resting-state functional MRI study. *Neuroreport* 2024;35(10):621-626.

25 Palejwala AH, Dadario NB, Young IM, *et al*. Anatomy and white matter connections of the lingual gyrus and cuneus. *World Neurosurg* 2021;151:e426-e437.

26 Xue KK, Chen JL, Wei YR, *et al*. Altered static and dynamic functional connectivity of habenula in first-episode, drug-naïve schizophrenia patients, and their association with symptoms including hallucination and anxiety. *Front Psychiatry* 2023;14:1078779.

27 Zhang CY, Lee TMC, Fu YW, *et al*. Properties of cross-modal occipital responses in early blindness: an ALE meta-analysis. *Neuroimage Clin* 2019;24:102041.

28 Proverbio AM, Camporeale E, Brusa A. Multimodal recognition of emotions in music and facial expressions. *Front Hum Neurosci* 2020;14:32.

29 Hong TY, Yang CJ, Cheng LK, *et al*. Enhanced white matter fiber tract of the cortical visual system in visual artists: implications for creativity. *Front Neurosci* 2023;17:1248266.

30 Abboud S, Cohen L. Distinctive interaction between cognitive networks and the visual cortex in early blind individuals. *Cereb Cortex* 2019;29(11):4725-4742.

31 He XY, Hong J, Liu ZH, *et al*. Decreased functional connectivity of the primary visual cortex and the correlation with clinical features in patients with intermittent exotropia. *Front Neurol* 2021;12:638402.

32 Rudebeck PH, Rich EL. Orbitofrontal cortex. *Curr Biol* 2018;28(18):R1083-R1088.

33 Heather Hsu CC, Rolls ET, Huang CC, *et al*. Connections of the human orbitofrontal cortex and inferior frontal gyrus. *Cereb Cortex* 2020;30(11):5830-5843.

34 Münster A, Hauber W. Medial orbitofrontal cortex mediates effort-related responding in rats. *Cereb Cortex* 2018;28(12):4379-4389.

35 Rolls ET. The orbitofrontal cortex and emotion in health and disease, including depression. *Neuropsychologia* 2019;128:14-43.

36 Gore F, Hernandez M, Ramakrishnan C, *et al*. Orbitofrontal cortex control of striatum leads economic decision-making. *Nat Neurosci* 2023;26(9):1566-1574.

37 Andrewes DG, Jenkins LM. The role of the amygdala and the ventromedial prefrontal cortex in emotional regulation: implications for post-traumatic stress disorder. *Neuropsychol Rev* 2019;29(2):220-243.

38 Carlson JM, Cha J, Fekete T, *et al*. Left medial orbitofrontal cortex volume correlates with skydive-elicited euphoric experience. *Brain Struct Funct* 2016;221(8):4269-4279.

39 Jansen M, Overgaauw S, de Bruijn ERA. Social cognition and obsessive-compulsive disorder: a review of subdomains of social functioning. *Front Psychiatry* 2020;11:118.

40 Vandermeer MRJ, Liu P, Mohamed Ali O, *et al*. Orbitofrontal cortex grey matter volume is related to children's depressive symptoms. *NeuroImage Clin* 2020;28:102395.

41 Viering T, Hoekstra PJ, Philipsen A, *et al*. Emotion dysregulation and integration of emotion-related brain networks affect intraindividual change in ADHD severity throughout late adolescence. *Neuroimage* 2021;245:118729.

42 Briggs RG, Tanglay O, Dadario NB, *et al*. The unique fiber anatomy of middle temporal gyrus default mode connectivity. *Oper Neurosurg* 2021;21(1):E8-E14.

43 Timofeeva P, Finisguerra A, D'Argenio G, *et al*. Switching off: disruptive TMS reveals distinct contributions of the posterior middle temporal gyrus and angular gyrus to bilingual speech production. *Cereb Cortex* 2024;34(5):bhae188.

44 Xu JP, Wang JJ, Fan LZ, *et al*. Tractography-based parcellation of the human middle temporal gyrus. *Sci Rep* 2015;5:18883.

45 Chang EF, Raygor KP, Berger MS. Contemporary model of language organization: an overview for neurosurgeons. *J Neurosurg* 2015;122(2):250-261.

46 Davey J, Thompson HE, Hallam G, *et al*. Exploring the role of the posterior middle temporal gyrus in semantic cognition: Integration of anterior temporal lobe with executive processes. *Neuroimage* 2016;137:165-177.

47 Jackson RL, Cloutman LL, Lambon Ralph MA. Exploring distinct default mode and semantic networks using a systematic ICA approach. *Cortex* 2019;113:279-297.

48 Menon V. 20 years of the default mode network: a review and synthesis. *Neuron* 2023;111(16):2469-2487.

49 Xiao A, Ge QM, Zhong HF, *et al*. White matter hyperintensities of bilateral lenticular putamen in patients with proliferative diabetic retinopathy: a voxel-based morphometric study. *Diabetes Metab Syndr Obes* 2021;14:3653-3665.

50 Catani M. The anatomy of the human frontal lobe. *Handb Clin Neurol* 2019;163:95-122.

51 Putnam PT, Chang SWC. Social processing by the primate medial frontal cortex. *Int Rev Neurobiol* 2021;158:213-248.

52 Ninomiya T, Noritake A, Kobayashi K, *et al*. A causal role for frontal cortico-cortical coordination in social action monitoring. *Nat Commun* 2020;11(1):5233.

53 Friedman NP, Robbins TW. The role of prefrontal cortex in cognitive control and executive function. *Neuropsychopharmacology* 2022;47(1):72-89.

54 Martinez-Trujillo J. Visual attention in the prefrontal cortex. *Annu Rev Vis Sci* 2022;8:407-425.

55 Herbet G, Duffau H. Contribution of the medial eye field network to the voluntary deployment of visuospatial attention. *Nat Commun* 2022;13(1):328.

56 Huang ZX, Cai JH. Progress in brain magnetic resonance imaging of individuals with prader-willi syndrome. *J Clin Med* 2023;12(3):1054.

57 Zhang Q, Weber MA, Narayanan NS. Medial prefrontal cortex and the temporal control of action. *Int Rev Neurobiol* 2021;158:421-441.

58 Sachdev PS. The default mode network, depression and Alzheimer's disease. *Int Psychogeriatr* 2022;34(8):675-678.

59 Buckner RL, DiNicola LM. The brain's default network: updated anatomy, physiology and evolving insights. *Nat Rev Neurosci* 2019;20(10):593-608.

60 Smith V, Duncan J, Mitchell DJ. Roles of the default mode and multiple-demand networks in naturalistic versus symbolic decisions. *J Neurosci* 2021;41(10):2214-2228.

61 Zhou HX, Chen X, Shen YQ, *et al*. Rumination and the default mode network: meta-analysis of brain imaging studies and implications for depression. *Neuroimage* 2020;206:116287.

62 Yuan QQ, Qi WZ, Xue C, *et al*. Convergent functional changes of default mode network in mild cognitive impairment using activation likelihood estimation. *Front Aging Neurosci* 2021;13:708687.

63 Hu JY, Shu HY, Li QY, *et al*. Alternation of brain intrinsic activity in patients with hypertensive retinopathy: a resting-state fMRI study. *Aging* 2021;13(17):21659-21670.